Journal of Organometallic Chemistry, 379 (1989) 311–323
Elsevier Sequoia S.A., Lausanne – Printed in The Netherlands
JOM 20290

Chiral modification of trinuclear ruthenium clusters with proline and cysteine derivatives. Synthesis, crystal structure, and catalytic properties of $[(\mu_2\text{-H})Ru_3(CO)_{10}(\mu_2,\eta^2\text{-OCNCH}_2CH_2CH_2CHCH_2OCH_3)]$ and $[(\mu_2\text{-H})Ru_3(CO)_9(\mu_3,\eta^2\text{-N=CCH}_2CH_2CHCH_2OCH_3)]$

Georg Süss-Fink *, Thomas Jenke, Heike Heitz,

Institut für Anorganische Chemie der Rheinisch-Westfälischen Technischen Hochschule Aachen, Templergraben 55, D-5100 Aachen (F.R.G.)

Maria Angela Pellinghelli and Antonio Tiripicchio

Istituto di Chimica Generale ed Inorganica, Università di Parma, Centro di Studio per la Strutturistica Diffrattometrica del C.N.R., Viale delle Scienze, I-43100 Parma (Italy)

(Received July 7th, 1989)

Abstract

Proline and cysteine derivatives have been used for the chiral modification of the trinuclear ruthenium cluster system. Whereas proline derivatives yield carbamoyl Ru_3 clusters by N–H activation, the cysteine derivatives react by S–H activation to give mercapto Ru_3 clusters. The chiral methoxymethyl pyrrolydine carbamoyl clusters catalyse the enantioselective isomerization of nerol to give citronellal with an enantiomeric excess of 12.4%. The structures of $[(\mu_2\text{-H})Ru_3(CO)_{10}(\mu_2,\eta^2\text{-OCNCH}_2CH_2CH_2CHCH_2OCH_3)]$ (*R*-**2**) and $[(\mu_2\text{-H})Ru_3(CO)_9(\mu_3,\eta^2\text{-N=CCH}_2CH_2CHCH_2OCH_3)]$ (*S*-**3**) have been determined by X-ray diffraction methods. Crystals of *R*-**2** are monoclinic, space group $P2_1$ with $Z = 2$, in a unit cell of dimensions $a = 8.662(4)$, $b = 18.234(4)$, $c = 7.662(2)$ Å, $\beta = 94.87(2)°$. Crystals of *S*-**3** are monoclinic, space group $P2_1$ with $Z = 2$ in a unit cell of dimensions $a = 8.881(4)$, $b = 16.720(6)$, $c = 7.567(3)$ Å, $\beta = 112.15(2)°$. Both structures have been solved by direct and Fourier methods and refind by full-matrix least-squares to $R = 0.0581$ (*R*-**2**) and $R = 0.0239$ (*S*-**3**) for 2366 (*R*-**2**) and 2454 (*S*-**3**) observed reflections. The structure of *R*-**2** consists of a ruthenium triangle of unequal edges with both the hydride and carbamoyl ligands bridging the longest edge; the

* Author to whom correspondence should be addressed. Present address: Institut de Chimie, Université de Neuchâtel, Avenue de Bellevaux 51, CH-2000 Neuchâtel (Suisse)

0022-328X/89/$03.50

carbamoyl ligand interacts through the carbon and oxygen atoms. The structure of *S*-**3** shows a metal triangle of unequal edges in which the dehydrogenated substituted pyrrolidine ligand interacts with all three Ru atoms through the C and N atoms of the imine group to form two σ-bonds with the two metals defining the longest edge (bridged also by the hydride ligand) and a π-bond with the third one.

Introduction

Transition-metal clusters have received much attention because it is hoped that they may provide more selective catalytic systems than those based on mononuclear transition-metal complexes [1,2]. Excellent chemo- and regio-selectivity were obtained in the hydroformylation of propylene with the cluster anion $[HRu_3(CO)_{11}]^-$ as catalyst [3–5]. In order to employ transition-metal clusters as enantioselective catalysts, chiral diphosphine ligands have been introduced into various ruthenium clusters: with (+)-(4*R*,5*R*)-4,5-bis(diphenylphosphinomethyl)-2,2-dimethyl-1,3-dioxolan (*R*,*R*-DIOP) the di-, tri-, tetra- and hexanuclear ruthenium clusters $Ru_2(CO)_4(OOCR)_2$(*R*,*R*-DIOP) [6], $Ru_3(CO)_{10}$(*R*,*R*-DIOP) [7], $H_4Ru_4(CO)_8$-(*R*,*R*-DIOP)$_2$ [8] and $Ru_6(CO)_{18}$(*R*,*R*-DIOP)$_3$ [9] have been synthesised. In this paper we report the chiral modification of the trinuclear ruthenium system with ligands derived from the chiral pool of proline and cysteine derivatives.

Results and discussion

The proline derivatives *S*-proline methylester as well as *S*- and *R*-methoxymethyl pyrrolidine react with $Ru_3(CO)_{12}$ at 50 °C in the presence of a catalytic amount of sodium and benzophenone to give the μ_2,η^2-carbamoyl clusters *S*-**1**, *S*-**2** and *R*-**2**, respectively. In the case of the methoxymethyl pyrrolidines the μ_3,η^2-imino clusters *S*-**3** and *R*-**3** are formed as by-products; they can be made the main products by carrying out the reaction in concentrated solutions. The compounds are obtained as air-stable yellow crystals from methanol after separation by preparative thin-layer chromatography.

The clusters *S*-**1**, *S*-**2** and *R*-**2** are characterized in the mass spectra by their molecular ions and characteristic fragments ions due to subsequent loss of carbonyl ligands; the peaks exhibit the typical Ru_3 isotopic pattern. The infrared spectra (Table 1) show the ν(CO) absorption pattern expected for the ten carbonyls of a $Ru_3(CO)_{10}$ framework containing two μ_2-bridging ligands. In the ^{1}H NMR spectra (Table 1) the signals of the organic ligand are easily identified by comparison with the spectra of the non-coordinated proline derivative; the resonances of the μ_2-hydride ligand show up at e.g. −14 ppm. In contrast that of *S*-**1**, which gives only one hydride signal, the spectra of both, *S*-**2** and *R*-**2**, reveal the presence of two hydride signals in an approximate 3/1 ratio. The appearance of these two hydride signals can only be accounted for by assuming the existence of two isomers (**a** and **b**) in solution, these being distinguished by different orientations of the carbamoyl bridge. Since the ^{1}H NMR spectra of *S*-**2** and *R*-**2** show no temperature dependance over the range −80 to +60 °C as far as the intensity ratio of the hydride signals is concerned, the two hydride signals cannot be accounted for in terms of a fluxional process. The existence of two stereoisomers due to different orientations of the

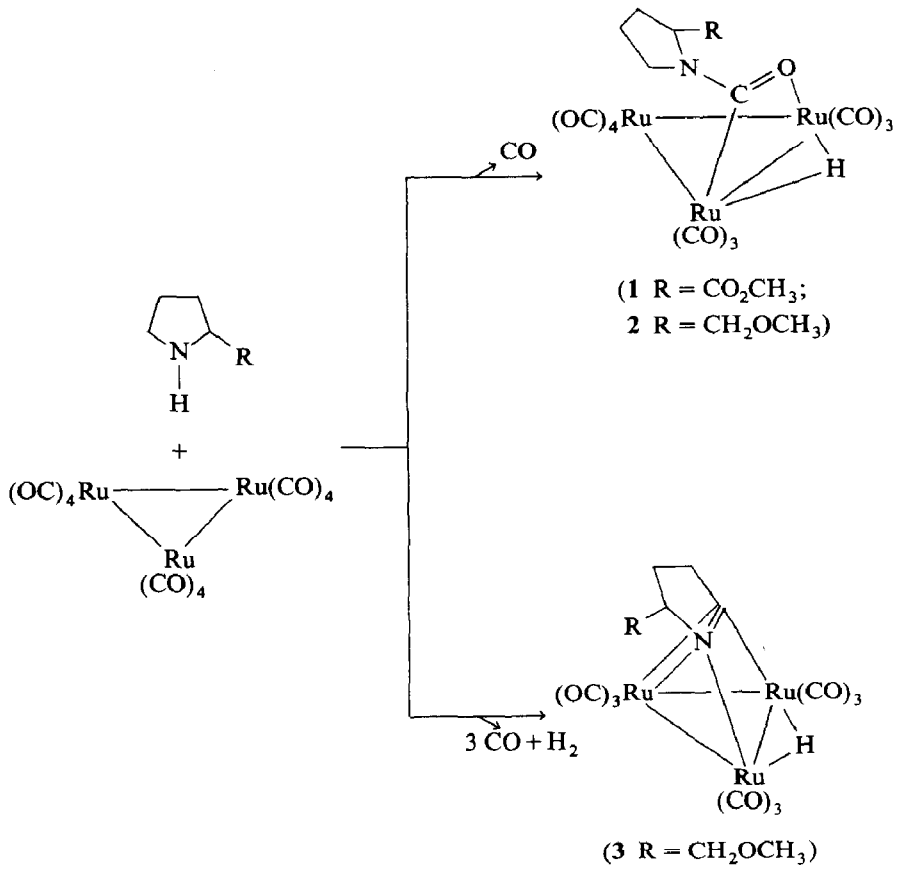

chiral μ_2-bridge has also been observed for $[(\mu_2\text{-H})Os_3(CO)_{10}(\mu_2,\eta^2\text{-OC-NHCHMePh})]$ [10]. Efforts to separate the stereoisomers *S*-**2** and *R*-**2** by chromatography failed, however, and in the solid state (see underneath) only one stereoisomer was found. It is not yet clear why solutions of **2** seem to contain two stereoisomers, whereas for **1** and **3** the NMR spectra indicate the existence of only one stereoisomer.

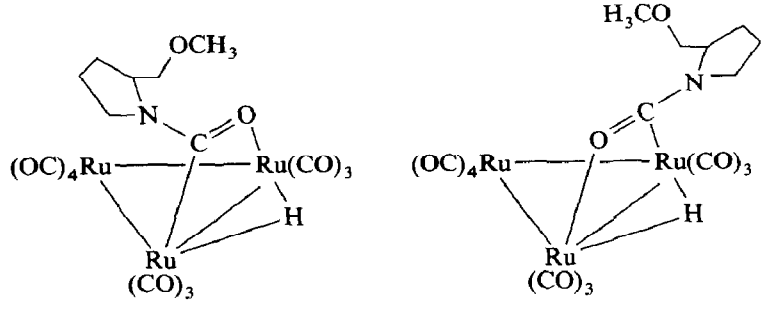

Table 1

IR and NMR data for the clusters **1** and **2** (*R* and *S* enantiomers)

	IR [a] ν(CO) (cm^{-1})	^{1}H-NMR [b] δ (ppm)
S-**1**	2095w, 2060vs, 2045vs, 2020s, 2010s, 2000m, 1995m, 1980vw, 1752vw	4.38 (1H); 3.77 (1H); 3.73 (1H); 3.66 (3H); 2.88 (1H); 2.48 (1H); 2.15 (1H); 2.01 (1H); −14.15 (1H)
S-**2**	2100m, 2062s, 2051vs, 2022s, 2014s, 1997m	4.15–3.20 (m,7H); 1.30 (m, 4H); 1.50 (s,1H); −13.85, −14.01 (2s,1H);
R-**2**	2100m, 2062s, 2050vs, 2023s, 2014s, 1998m	4.14–3.19 (m,7H); 1.30 (m,4H); 1.50 (s,1H); −13.84, −14.01 (2s,1H)
S-**3**	2090m, 2060s, 2032vs, 2010vs, 2002m sh, 2000m, 1998m sh, 1971m	3.60–2.93 (m,7H); 1.81–1.27 (m,5H); −18.29 (s,1H)
R-**3**	2090m, 2062s, 2032vs, 2011vs, 2002m sh, 2000m, 1998m sh, 1972m	3.61–2.93 (m,7H); 1.82–1.24 (m,5H); −18.31 (s,1H)
S-**4**	2090m, 2045s, 2018vs, 2001s, 1985m, 1945m, 1745w	4.10 (q,2H); 3.47 (s,2H); 2.30–2.70 (m,3H); 1.24 (tr,3H); −14.52 (s,1H)

[a] In cyclohexane solution. [b] In $CDCl_3$ solution, 30 °C.

The clusters *S*-**1**, *S*-**2**, and *R*-**2** represent chiral analogues of [(μ_2-H)$Ru_3(CO)_{10}$(μ_2,η^2-OCNMe$_2$)], reported by Kaesz et al. as a product of the reaction of $Ru_3(CO)_{12}$ with dimethylamine [11].

Crystal structure of [(μ_2-H)$Ru_3(CO)_{10}$(μ_2,η^2-OC$\overline{NCH_2CH_2CH_2C}HCH_2OCH_3$)] (R-2)

The molecular structure of *R*-**2** is depicted in Fig. 1 together with the atomic numbering scheme; selected bond distances and angles are listed in Table 2. The molecule consists of a triangular cluster of Ru atoms with edges of unequal length, 2.897(2), 2.870(2) and 2.823(2) Å. The unique Ru(3) atom is linked to four terminal carbonyl groups, the remaining Ru(1) and Ru(2) atoms are linked to three terminal carbonyl groups and are bridged by both the hydride and the carbamoyl ligands, through the C(1) and O(1) atoms. The doubly-bridged Ru(1)–Ru(2) edge is the longest one. The hydride and the carbamoyl bridges are on opposite sides with respect to the triruthenium triangle. The dihedral angles formed by the Ru(1)–H(1)–Ru(2) and Ru(1)–C(1)–O(1)–Ru(2) bridges with the metal triangle are 118(3) and 103.8(2)°; the latter angle is mainly determind by the steric interaction between the carbamoyl bridge and the axial C(8)–O(8) carbonyl [C(1) · · · C(8) = 2.87(3) and O(1) · · · C(8) = 2.85(2) Å]. The rather large Ru(1)–Ru(2)–C(5) and Ru(2)–Ru(1)–C(3) angles, 113.0(5) and 115.5(6)°, are typical of the Ru–H–Ru system, and confirm the presence of the hydride bridging the Ru(1)–Ru(2) edge. The structure of *R*-**2** is strictly comparable with that of [(μ_2-H)$Os_3(CO)_{10}$(μ_2,η^2-OCNHCHMePh)] [10]. Furthermore the Ru(1)–C(1) and Ru(2)–O(1) distances, involving the carbamoyl ligand, in *R*-**2**, 2.10(2) and 2.09(1) Å are practically equal to those, namely 2.098(8) and 2.100(5) Å, for the triosmium cluster. The carbamoyl moiety is nearly planar, the maximum deviation from the mean plane passing through C(12), C(15), N, C(1), Ru(1) and O(1) being 0.05(2) Å for C(15). Within the

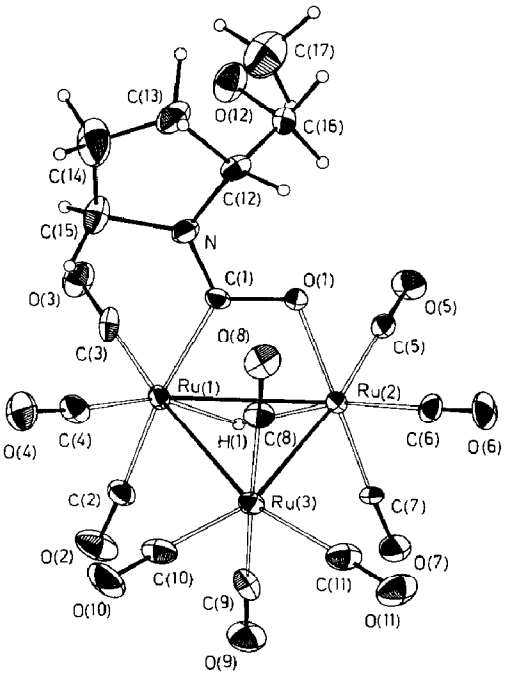

Fig. 1. View of the structure of $[(\mu_2\text{-H})Ru_3(CO)_{10}(\mu_2,\eta^2\text{-OC}\overline{NCH_2CH_2CH_2CH}CHCH_2OCH_3)]$ (*R*-**2**) with the atomic numbering scheme.

carbamoyl group the double bond can be regarded as delocalized over the C(1)–O(1) and C(1)–N bonds, as indicated by their bond lengths, 1.28(2) and 1.35(2) Å, so that its structure can be described in terms of a resonance between the two canonical structures represented below. The polar form is also consistent with the

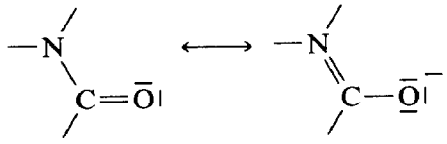

conformation around the C(12)–C(16) bond, showing the O(12) atom to be +synclinal and at a rather short distance [N · · · O(12) = 2.87(2) Å] with respect to the nitrogen atom. This conformation should be the less favoured in terms solely of steric hindrance effects. The conformation of the pentaatomic pyrrolidine ring is "twist" around the C(12)–C(13) bond.

The mass spectra of complexes *S*-**3** and *R*-**3** show only a small molecular peak with the Ru_3 isotope pattern, and the fragmentation is determined by the subsequent loss of carbonyl ligands. The IR and NMR data (Table 1) are consistent with the presence of a μ_2-hydride, nine terminal carbonyls, and a triply-bridging imino ligand. The C=N stretching frequency, however, cannot be assigned unambiguously to one of the absorptions in the infrared spectra.

Crystal structure of $[(\mu_2\text{-}H)Ru_3(CO)_9(\mu_3,\eta^2\text{-}\overline{N{=}CCH_2CH_2CH}CHCH_2OCH_3)]$ (*S*-**3**)

The molecular structure of *S*-**3** is shown in Fig. 2 together with the atomic numbering scheme; selected bond distances and angles are listed in Table 3. The structure consists of a triangular cluster of Ru atoms with unequal bond lengths,

Table 2

Selected bond distances (Å) and angles (°) in *R*-**2**

Ru(1)–Ru(2)	2.897(2)	Ru(2)–C(6)	1.96(2)
Ru(1)–Ru(3)	2.870(2)	Ru(2)–C(7)	1.90(6)
Ru(2)–Ru(3)	2.823(2)	Ru(3)–C(8)	1.92(2)
Ru(1)–C(1)	2.10(2)	Ru(3)–C(9)	2.00(2)
Ru(2)–O(1)	2.09(1)	Ru(3)–C(10)	1.93(2)
C(1)–O(1)	1.28(2)	Ru(3)–C(11)	1.92(2)
N–C(1)	1.35(2)	C(2)–O(2)	1.13(2)
N–C(12)	1.46(2)	C(3)–O(3)	1.15(2)
N–C(15)	1.50(3)	C(4)–O(4)	1.15(3)
C(12)–C(13)	1.53(3)	C(5)–O(5)	1.15(2)
C(13)–C(14)	1.41(4)	C(6)–O(6)	1.10(3)
C(14)–C(15)	1.46(4)	C(7)–O(7)	1.13(2)
C(12)–C(16)	1.51(3)	C(8)–O(8)	1.15(2)
C(16)–O(12)	1.38(3)	C(9)–O(9)	1.09(3)
O(12)–C(17)	1.38(4)	C(10)–O(10)	1.12(3)
Ru(1)–C(2)	1.97(2)	C(11)–O(11)	1.13(3)
Ru(1)–C(3)	1.90(2)	Ru(1)–H(1)	1.91(10)
Ru(1)–C(4)	1.88(2)	Ru(2)–H(1)	2.04(11)
Ru(2)–C(5)	1.96(2)		
Ru(2)–Ru(1)–Ru(3)	58.62(5)	Ru(1)–Ru(3)–C(9)	87.2(6)
Ru(1)–Ru(2)–Ru(3)	60.20(5)	Ru(1)–Ru(3)–C(10)	97.5(7)
Ru(1)–Ru(3)–Ru(2)	61.17(5)	Ru(2)–Ru(3)–C(8)	86.2(6)
C(2)–Ru(1)–C(3)	92.7(8)	Ru(2)–Ru(3)–C(9)	86.5(6)
C(2)–Ru(1)–C(4)	91.6(8)	Ru(2)–Ru(3)–C(11)	98.6(7)
C(3)–Ru(1)–C(4)	100.3(9)	Ru(2)–O(1)–C(1)	109.2(9)
C(1)–Ru(1)–C(3)	89.3(7)	Ru(1)–C(1)–O(1)	116(1)
C(1)–Ru(1)–C(4)	96.8(8)	Ru(1)–C(1)–N	130(1)
Ru(2)–Ru(1)–C(1)	65.5(4)	O(1)–C(1)–N	114(1)
Ru(2)–Ru(1)–C(2)	105.7(6)	C(1)–N–C(12)	122(1)
Ru(2)–Ru(1)–C(3)	115.5(6)	C(1)–N–C(15)	126(2)
Ru(3)–Ru(1)–C(1)	88.5(4)	C(12)–N–C(15)	112(1)
Ru(3)–Ru(1)–C(2)	88.6(6)	N–C(12)–C(13)	103(2)
Ru(3)–Ru(1)–C(4)	85.4(6)	N–C(12)–C(16)	113(2)
C(5)–Ru(2)–C(6)	98.0(8)	C(13)–C(12)–C(16)	115(2)
C(5)–Ru(2)–C(7)	94.2(8)	C(12)–C(13)–C(14)	109(2)
C(6)–Ru(2)–C(7)	91.7(8)	C(13)–C(14)–C(15)	111(2)
O(1)–Ru(2)–C(5)	85.4(6)	C(14)–C(15)–N	104(2)
O(1)–Ru(2)–C(6)	89.4(7)	C(16)–O(12)–C(17)	114(2)
Ru(1)–Ru(2)–C(5)	113.0(5)	Ru(1)–C(2)–O(2)	177(2)
Ru(1)–Ru(2)–C(7)	110.1(5)	Ru(1)–C(3)–O(3)	179(2)
Ru(1)–Ru(2)–O(1)	69.1(3)	Ru(1)–C(4)–O(4)	176(2)
Ru(3)–Ru(2)–C(6)	87.7(6)	Ru(2)–C(5)–O(5)	175(1)
Ru(3)–Ru(2)–C(7)	89.5(5)	Ru(2)–C(6)–O(6)	179(2)
Ru(3)–Ru(2)–O(1)	90.8(3)	Ru(2)–C(7)–O(7)	176(2)
C(8)–Ru(3)–C(10)	93.0(9)	Ru(3)–C(8)–O(8)	179(2)
C(8)–Ru(3)–C(11)	91.7(9)	Ru(3)–C(9)–O(9)	170(2)
C(9)–Ru(3)–C(10)	93.0(9)	Ru(3)–C(10)–O(10)	179(2)
C(9)–Ru(3)–C(11)	91.4(9)	Ru(3)–C(11)–O(11)	178(2)
C(10)–Ru(3)–C(11)	102.7(10)	Ru(1)–H(1)–Ru(2)	94(4)
Ru(1)–Ru(3)–C(8)	87.5(6)		

2.971(1), 2.754(1) and 2.698(1) Å. Each Ru atom is bound to three terminal carbonyl groups. The longest edge of the cluster, Ru(1)–Ru(2), is bridged by both the hydride ligand and by the substituted pyrroline ligand, obtained by the oxidation of the

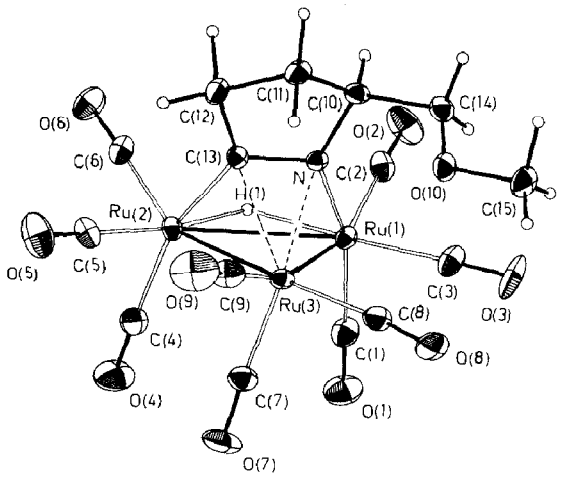

Fig. 2. View of the structure of $[(\mu_2\text{-H})Ru_3(CO)_9(\mu_3,\eta^2\text{-}\overline{N{=}CCH_2CH_2CHCH_2OCH_3})]$ (*S*-**3**) with the atomic numbering scheme.

starting pyrrolidine ligand, through the N and C(13) atoms [the Ru(1)–N and Ru(2)–C(13) bond lengths are 2.093(4) and 2.038(5) Å]. The hydride bridge is almost coplanar with the Ru triangle, the dihedral angle being 2(3)°, whereas the rather unsymmetrical Ru(1)–N–C(13)–Ru(2) bridge forms a dihedral angle of 60.9(1)°. In this case also the presence of the hydride on the Ru(1)–Ru(2) edge causes opening of the Ru(1)–Ru(2)–C(6) and Ru(2)–Ru(1)–C(2) angles [111.6(2) and 113.6(2)°]. The substituted Δ^1-pyrroline ligand interacts with all the Ru atoms, being involved also in a π bond, through the iminic N–C(13) bond, to the Ru(3) atom [Ru(3)–N and Ru(3)–C(13) distances are 2.230(4) and 2.275(6), Å, respectively]. It shows an "envelope" conformation with the C(11) atom bent towards the Ru(3) atom. The interaction of the N–C(13) bond with Ru(3) also determines the folding of the C(12)–C(13)–N–C(10) group with respect to the Ru(1)–N–C(13)–Ru(2) bridge (the dihedral angle being 169.0(2)°). The conformation around the C(10)–C(14) bond shows the O(10) atom to be −synclinal with respect to the nitrogen atom, even if at a longer distance than in *R*-**2** [N ··· O(10) = 3.031(6) Å].

Cysteine derivatives react by S–H activation instead of N–H activation. The reaction of *S*-cysteine ethyl-ester with $Ru_3(CO)_{12}$ at 60°C in the presence of sodium-benzophenone as catalyst results in the formation of the cluster $[(\mu_2\text{-H})Ru_3(CO)_9(\mu_3,\eta^2\text{-}SCH_2CH(NH_2)CO_2CH_2CH_3)]$ (*S*-**4**). The compound was isolated as an orange crystalline material by preparative thin-layer chromatography.

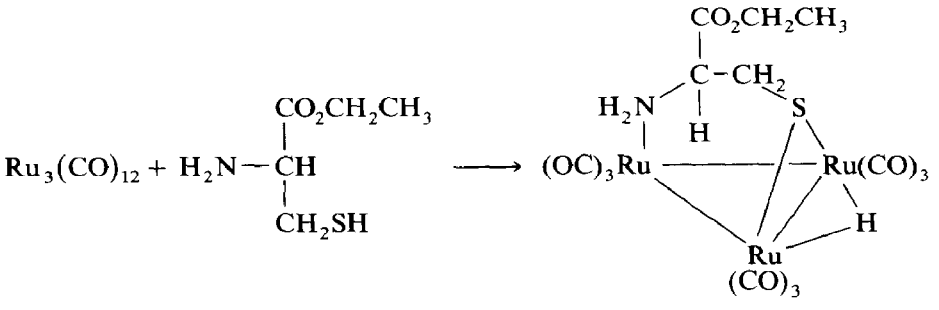

(*S*-**4**)

Table 3

Selected bond distances (Å) and angles (°) in *S*-3

Ru(1)–Ru(2)	2.971(1)	Ru(2)–C(4)	1.964(8)
Ru(1)–Ru(3)	2.698(1)	Ru(2)–C(5)	1.889(6)
Ru(2)–Ru(3)	2.754(1)	Ru(2)–C(6)	1.916(8)
Ru(1)–N	2.093(4)	Ru(3)–C(7)	1.877(7)
Ru(2)–C(13)	2.038(5)	Ru(3)–C(8)	1.919(8)
Ru(3)–N	2.230(4)	Ru(3)–C(9)	1.908(8)
Ru(3)–C(13)	2.275(6)	C(1)–O(1)	1.154(11)
N–C(13)	1.349(6)	C(2)–O(2)	1.131(9)
N–C(10)	1.497(7)	C(3)–O(3)	1.123(10)
C(10)–C(11)	1.522(8)	C(4)–O(4)	1.134(11)
C(11)–C(12)	1.543(8)	C(5)–O(5)	1.127(9)
C(12)–C(13)	1.528(9)	C(6)–O(6)	1.135(11)
C(10)–C(14)	1.513(9)	C(7)–O(7)	1.153(10)
C(14)–O(10)	1.381(9)	C(8)–O(8)	1.145(11)
O(10)–C(15)	1.436(9)	C(9)–O(9)	1.129(11)
Ru(1)–C(1)	1.899(8)	Ru(1)–H(1)	1.85(10)
Ru(1)–C(2)	1.949(7)	Ru(2)–H(1)	1.78(8)
Ru(1)–C(3)	1.907(7)		
Ru(2)–Ru(1)–Ru(3)	57.87(3)	Ru(1)–Ru(3)–C(7)	96.8(2)
Ru(1)–Ru(2)–Ru(3)	56.09(3)	Ru(1)–Ru(3)–C(8)	97.5(2)
Ru(1)–Ru(3)–Ru(2)	66.04(3)	Ru(2)–Ru(3)–C(7)	81.3(2)
C(1)–Ru(1)–C(2)	96.8(3)	Ru(2)–Ru(3)–C(9)	104.8(3)
C(1)–Ru(1)–C(3)	90.1(3)	C(10)–N–C(13)	110.3(4)
C(2)–Ru(1)–C(3)	93.8(3)	Ru(1)–N–C(10)	136.7(4)
N–Ru(1)–C(2)	103.9(2)	Ru(1)–N–C(13)	110.6(3)
N–Ru(1)–C(3)	96.4(2)	N–C(10)–C(11)	103.6(5)
Ru(2)–Ru(1)–C(1)	97.5(2)	N–C(10)–C(14)	115.3(5)
Ru(2)–Ru(1)–C(2)	113.6(2)	C(11)–C(10)–C(14)	117.1(5)
Ru(2)–Ru(1)–N	67.0(1)	C(10)–C(11)–C(12)	102.6(5)
Ru(3)–Ru(1)–C(1)	105.0(2)	C(11)–C(12)–C(13)	103.1(5)
Ru(3)–Ru(1)–C(3)	92.4(2)	C(12)–C(13)–N	109.9(5)
Ru(3)–Ru(1)–N	53.7(1)	Ru(2)–C(13)–N	115.6(4)
C(4)–Ru(2)–C(5)	93.7(3)	Ru(2)–C(13)–C(12)	134.1(4)
C(4)–Ru(2)–C(6)	96.0(3)	C(10)–C(14)–O(10)	110.4(5)
C(5)–Ru(2)–C(6)	94.6(3)	C(14)–O(10)–C(15)	112.7(5)
C(13)–Ru(2)–C(5)	91.6(3)	Ru(1)–C(1)–O(1)	178.5(7)
C(13)–Ru(2)–C(6)	100.7(2)	Ru(1)–C(2)–O(2)	178.0(7)
Ru(1)–Ru(2)–C(4)	101.0(2)	Ru(1)–C(3)–O(3)	178.0(8)
Ru(1)–Ru(2)–C(6)	111.6(2)	Ru(2)–C(4)–O(4)	178.0(8)
Ru(1)–Ru(2)–C(13)	66.7(2)	Ru(2)–C(5)–O(5)	179.1(7)
Ru(3)–Ru(2)–C(4)	108.3(2)	Ru(2)–C(6)–O(6)	177.5(6)
Ru(3)–Ru(2)–C(5)	92.5(2)	Ru(3)–C(7)–O(7)	176.2(7)
Ru(3)–Ru(2)–C(13)	54.2(2)	Ru(3)–C(8)–O(8)	175.2(6)
C(7)–Ru(3)–C(8)	96.4(3)	Ru(3)–C(9)–O(9)	178.9(8)
C(7)–Ru(3)–C(9)	97.5(3)	Ru(1)–H(1)–Ru(2)	110(5)
C(8)–Ru(3)–C(9)	92.5(3)		

The transfer of the hydride from the sulfur and not from the nitrogen is confirmed by the absence of the ν(SH) absorption and the SH proton resonance in the IR and NMR spectra of *S*-4. The presence of the intact NH_2 group is revealed by three ν(NH) absorptions at 3355, 3340, and 3300 cm^{-1}; the ν(CO) pattern of the

infrared spectra (Table 1) suggests a $Ru_3(CO)_9$ arrangement similar to that in *S*-**3** and *R*-**3**. The ^1H NMR data (Table 1) and the mass spectrum (Ru_3 pattern, molecular ion $m/e = 707$, fragments due to the loss of 1–2 H and 1–9 CO) are in accord with the structure proposed for *S*-**4**. A similar S–H activation has been observed in the reaction of $Ru_3(CO)_{12}$ with thiols [12] and with mercaptoacetic acid [13]. However, an isomeric structure in which the NH_2 moiety is coordinated to one of the bridgehead ruthenium atoms, and not to the unbridged one, cannot be excluded for *S*-**4** on the basis of the spectroscopic data.

The chiral cluster **2** catalyses the isomerization of the prochiral allylic alcohol nerol to give the chiral aldehyde citronellal. The reaction proceeds at 60 °C, and also yields geraniol, the *trans* isomer of nerol, as a side-product. Both the catalytic turnover (41 mol citronellal per mol catalyst) and the enantiomeric excess (12.4%) are rather modest, but prove that optical induction by the chiral ligand in **2** is part of the catalytic properties of this cluster. A side-reaction catalysed by **2** involves the *cis-trans* isomerization of nerol to give geraniol.

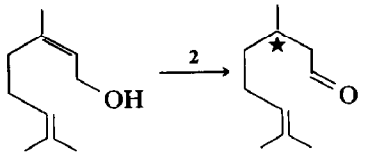

nerol citronellal

The enantiomeric excess was determined by treatment of the citronellal enantiomers with (*S*)-1-amino-2-methoxymethyl pyrrolidine (SAMP) to give the diastereomeric hydrazones, which can be separated by GLC [14].

Experimental

The reactions were carried out under dry nitrogen in anhydrous and N_2-saturated solvents. Preparative thin-layer chromatography was performed on plates covered with ICN Silica GF–DC 60 A. The spectra were recorded on a Perkin–Elmer IR spectrometer 580 and a Bruker NMR spectrometer WP 80. The GLC separation of the diastereomeric hydrazones was performed on a Siemens Sichromat 3 with a 75 m × 0.25 mm fused silica capillary column based on cyclodextrine. SAMP was prepared according by published methods [15].

Synthesis of the aminoacid esters

A solution of 0.4 mmol (0.3 mmol) potassium hydroxide in 5 ml methanol and aminoacid ester hydrochloride [proline methylester hydrochloride: 66.2 mg (0.4 mmol); cysteine ethylester hydrochloride: 55.7 mg (0.3 mmol)] was stirred for 0.5 h. After filtration through anhydrous Na_2SO_4 the solution was used for the reaction with ruthenium carbonyl.

Synthesis of ***1, 2 and 4***

To a solution of 160 mg (0.25 mmol) $Ru_3(CO)_{12}$ in 40 ml THF was added an excess of the aminoacid derivative (proline methylester: 0.4 mmol, methoxymethyl pyrrolidine: 1 mmol, cysteine ethylester: 0.3 mmol). After addition of 4 drops of a solution of sodium-benzophenone in THF [15,16] the mixture was stirred at elevated

temperature (**1**: 50 °C, 18 h; **2** and **4**: 60 °C, 20 h). Then the solvent was drawn off, the residue was taken up into 5 ml CH_2Cl_2 and subjected to thin-layer chromatography with CH_2Cl_2/cyclohexane (**1** and **4**: 30/70, **2**: 40/60) as eluant. The products were extracted from the yellow main band (**2**: third band) with CH_2Cl_2 and recrystallized from methanol.

1 $C_{17}H_{11}NO_{13}Ru_3$ (740.5), yield 91 mg (49%), m.p.: 114 °C (dec.). Found: C, 27.32; H, 1.49; N, 1.87. Calcd: C, 27.58; H, 1.50; N, 1.89%.

2 $C_{17}H_{13}NO_{12}Ru_3$ (726.5), yield 99 mg (54%), m.p.: 109 °C (dec.). Found: C, 27.51; H, 1.88; N, 2.00. Calcd: C, 28.11; H, 1.80; N, 1.93%.

4 $C_{14}H_{11}NORu_3S$ (704.5), yield 137 mg (78%), m.p.: 148 °C (dec.). Found: C, 23.41; H, 1.59; N, 2.12. Calcd: C, 23.87; H, 1.58; N, 1.99%.

Synthesis of 3

To a suspension of 160 mg (0.25 mmol) $Ru_3(CO)_{12}$ in 10 ml THF was added an excess of methoxymethylpyrrolidine (0.47 mmol). After 0.5 h the solvent was removed and the residue was taken up into 3 ml THF. The product was separated by TLC (cyclohexane/CH_2Cl_2 6 : 4), extracted from the orange main band with ether, and recrystallized from ethanol.

3 $C_{15}H_{11}NO_{10}Ru_3$ (668.5), yield 108 mg (61%), m.p.: 168 °C (dec.). Found: C, 26.87; H, 1.95; N, 2.09. Calcd: C, 26.95; H, 1.66; N, 2.10.

Isomerization of nerol to citronellal

A solution of 50 mg of (0.07 mmol) **2** and 2 ml (11.2 mmol) of nerol in 10 ml THF was stirred at 60 °C. After 20 h the mixture was distilled (10 mbar, 100 °C bath temperature) and the fraction of b.p. 85–88 °C, which contained the citronellals, was dissolved in 10 ml of cyclohexane. To this solution cooled to 0 °C, 0.39 ml (3 mmol) of the hydrazine SAMP was added dropwise. The solution was allowed to warm up the room temperature and after 1 h filtered through anhydrous Na_2SO_4 and used in this form for GLC analysis of the diastereomeric hydrazones.

Crystal structure determinations of $[(\mu_2\text{-}H)Ru_3(CO)_{10}(\mu_2,\eta^2\text{-}OC\overline{NCH_2CH_2CH_2CH}C\text{-}H_2OCH_3)]$ *(R-2) and of* $[(\mu_2\text{-}H)Ru_3(CO)_9(\mu_3,\eta^2\text{-}\overline{N{=}CCH_2CH_2CH}CHCH_2OCH_3]$ *(S-3)*

Yellow crystals of approximate dimensions 0.15 × 0.25 × 0.30 (*R*-**2**) and 0.18 × 0.22 × 0.35 mm (*S*-**3**) were used for the X-ray analyses.

Crystal data. *R*-**2**: $C_{17}H_{13}NO_{12}Ru_3$, $M = 726.50$, monoclinic, space group $P2_1$, $a = 8.662(4)$, $b = 18.234(4)$, $c = 7.662(2)$ Å, $\beta = 94.87(2)°$, $V = 1205.8(7)$ Å^3 (by least-squares refinement from the θ values of 30 accurately measured reflections, $\bar{\lambda} = 0.71073$ Å), $Z = 2$, $D_c = 2.001$ g cm^{-3}, $F(000) = 700$, μ(Mo-K_α) = 18.77 cm^{-1}.

S-**3**: $C_{15}H_{11}NO_{10}Ru_3$, $M = 668.46$, monoclinic, space group $P2_1$, $a = 8.881(4)$, $b = 16.720(6)$, $c = 7.567(3)$ Å, $\beta = 112.15(2)°$, $V = 1040.7(7)$ Å^3 (by least-squares refinement from the θ values of 30 accurately measured reflections, $\bar{\lambda} = 0.71073$ Å, $Z = 2$, $D_c = 2.133$ g cm^{-3}, $F(000) = 640$, μ(Mo-K_α) = 21.59 cm^{-1}.

Data collection and processing. A Siemens AED single-crystal diffractometer ($\theta/2\theta$ scan mode, niobium-filtered Mo-K_α radiation) was employed. All reflections with θ in the range 3–27 ° for both *R*-**2** and *S*-**3** were measured; of 2917 (*R*-**2**) and 2522 (*S*-**3**) independent reflections, 2366 (*R*-**2**) and 2454 (*S*-**3**), having $I \geq 2\sigma(I)$, were considered observed and used in the analyses.

Structure solutions and refinements. Direct and Fourier methods were used with full-matrix least-squares refinements with anisotropic thermal parameters in the last cycles for all the non-hydrogen atoms. In order to confirm the absolute configuration of both compounds independent final cycles of refinement were carried out using the coordinates $-x, -y, -z$ for all the non-hydrogen atoms. A slight increase in the R value was obtained for both *R*-**2** and *S*-**3** [$R(x, y, z) = 0.0651$, $R(-x, -y, -z) = 0.0665$ and $R(x, y, z) = 0.0258$, $R(-x, -y, -z) = 0.0271$ respectively. All the hydrogen atoms of *R*-**2** except for the hydride H(1) (which was clearly located in the final difference Fourier map) were placed at calculated positions (C–H = 1.08 Å) and refined riding on the corresponding carbon atoms. All the hydrogen atoms of *S*-**3** were clearly located in the final difference Fourier map, but not refined, except for hydride H(1). In both cases all hydrogen atoms were introduced in the final structure factors calculations. For both structures a weighting scheme $w =$

Table 4

Fractional atomic coordinates ($\times 10^4$) (with e.s.d.'s in parentheses) for the non-hydrogen atoms of complex *R*-**2**

Atom	x/a	y/b	z/c
Ru(1)	4812(1)	0	1162(2)
Ru(2)	2391(1)	1100(1)	1028(2)
Ru(3)	4486(1)	977(1)	4043(2)
O(1)	1498(10)	60(6)	1479(14)
O(2)	7826(7)	799(10)	383(21)
O(3)	4880(18)	−956(8)	−2094(20)
O(4)	6539(21)	−1015(10)	3781(27)
O(5)	341(16)	1088(9)	−2496(16)
O(6)	48(16)	1762(10)	3351(22)
O(7)	3669(16)	2600(8)	234(22)
O(8)	2206(18)	−138(8)	5363(17)
O(9)	6614(16)	2107(9)	2445(25)
O(10)	7198(9)	399(11)	6457(28)
O(11)	3256(21)	2212(10)	6242(25)
O(12)	−97(21)	−1607(10)	−1104(22)
N	2115(18)	−1110(8)	1650(22)
C(1)	2594(17)	−412(9)	1509(21)
C(2)	6717(20)	527(11)	693(27)
C(3)	4864(21)	−588(10)	−873(25)
C(4)	5908(22)	−607(12)	2827(25)
C(5)	1047(17)	1076(10)	−1162(22)
C(6)	903(24)	1524(10)	2529(26)
C(7)	3226(18)	2037(19)	581(27)
C(8)	3048(22)	285(10)	4873(27)
C(9)	5835(21)	1681(12)	2864(27)
C(10)	6195(25)	605(12)	5578(29)
C(11)	3684(26)	1754(13)	5407(30)
C(12)	504(22)	−1300(9)	1863(25)
C(13)	618(33)	−2103(11)	2462(39)
C(14)	2120(34)	−2366(18)	2231(65)
C(15)	3144(26)	−1769(11)	1807(32)
C(16)	−553(22)	−1162(11)	222(31)
C(17)	−708(46)	−1403(21)	−2752(51)

Table 5

Fractional atomic coordinates ($\times 10^4$) (with e.s.d.'s in parentheses) for the non-hydrogen atoms of complex *S*-**3**

Atom	*x/a*	*y/b*	*z/c*
Ru(1)	4744(1)	1066(1)	3399(1)
Ru(2)	1149(1)	1136(1)	1463(1)
Ru(3)	3065(1)	0	698(1)
O(1)	5514(9)	2425(4)	1178(10)
O(2)	6084(9)	1870(4)	7351(8)
O(3)	7965(6)	289(4)	3918(12)
O(4)	796(11)	2560(4)	−1281(12)
O(5)	−1935(8)	325(4)	−1103(10)
O(6)	−468(7)	1941(3)	3909(9)
O(7)	2541(9)	1051(4)	−2743(8)
O(8)	5949(8)	−881(4)	313(8)
O(9)	709(11)	−1314(5)	−1402(12)
O(10)	5657(5)	−1426(3)	3988(6)
N	3587(5)	35(3)	3820(5)
C(1)	5241(8)	1915(4)	2040(11)
C(2)	5564(7)	1580(4)	5895(10)
C(3)	6772(8)	570(4)	3756(12)
C(4)	898(9)	2042(4)	−276(10)
C(5)	−789(8)	634(4)	−148(10)
C(6)	165(7)	1650(4)	3023(10)
C(7)	2710(9)	669(4)	−1412(9)
C(8)	4898(9)	−559(4)	540(9)
C(9)	1596(11)	−831(5)	−610(11)
C(10)	4012(7)	−651(3)	5194(8)
C(11)	2531(8)	−1194(4)	4421(10)
C(12)	1129(7)	−594(4)	3526(10)
C(13)	1959(5)	104(3)	2954(7)
C(14)	5654(7)	−1029(4)	5587(9)
C(15)	7177(8)	−1815(5)	4298(12)

$K[\sigma^2(F_o) + gF_o^2]^{-1}$ was used in the last cycles of refinement with $K = 1.522$ (*R*-**2**) and 1.334 (*S*-**3**) and $g = 0.0011$ (*R*-**2**) and 0.0007 (*S*-**3**). Final R and R' values were 0.0581 and 0.0667 (*R*-**2**) and 0.0239 and 0.0322 (*S*-**3**) respectively. The SHELX system of computer programs was used [17]. Atomic scattering factors, corrected for anomalous dispersion, were taken from ref. 18. Final atomic coordinates for the non hydrogen atoms of *R*-**2** and *S*-**3** are given in Tables 4 and 5 respectively. All calculations were carried out on the CRAY X-MP/12 computer of the Centro di Calcolo Elettronico Interuniversitario dell'Italia Nord-Orientale, Bologna and on the GOUD POWERNODE 6040 computer of the Centro di Studio per la Strutturistica Diffrattometrica del C.N.R., Parma.

Lists of H-atom coordinates, thermal parameters, and remaining bond distances and angles for both structures are available from the authors.

Acknowledgments

Financial support by the Stiftung Volkswagenwerk, the Karl-Winnacker-Stiftung, the Fonds der chemischen Industrie and der Minister für Forschung und Wissen-

schaft des Landes Nordrhein-Westfahlen is gratefully acknowledged. The authors thank the Johnson Matthey Technology Centre for a loan of $RuCl_3 \cdot nH_2O$, and Dr. W. Meltzow, Institut für Technische Chemie und Petrolchemie der RWTH Aachen, for assistance in the GLC analysis of the diastereomeric isomers.

References

1 E.L. Muetterties, Bull. Soc. Chim. Belg., 84 (1975) 959.
2 B.F.G. Johnson and J. Lewis, Pure and Appl. Chem., 44 (1975) 43.
3 B.F.G. Johnson, J. Lewis, P.R. Raithby and G. Süss(-Fink), J. Chem. Soc., Dalton Trans., (1979) 1356.
4 G. Süss-Fink, Inorg. Synth., 24 (1986) 168.
5 G. Süss-Fink and G.F. Schmidt, J. Mol. Catal., 42 (1987) 361.
6 M. Bianchi, P. Frediani, U. Matteoli, G. Menchi, F. Piacenti and G. Petrucci, J. Organomet. Chem., 259 (1983) 207.
7 G. Süss-Fink and H. Jungbluth, J. Organomet. Chem., 352 (1988) 185.
8 M. Bianchi, F. Piacenti, P. Frediani, U. Matteoli, C. Botteghi, S. Gladiani and E. Benedetti, J. Organomet. Chem., 141 (1977) 107.
9 C. Botteghi and M. Bianchi, J. Organomet. Chem., 140 (1977) 221.
10 A.J. Arce and A.J. Deeming, J. Chem. Soc., Chem. Commun., (1980) 1102.
11 R. Szostak, C.E. Strouse and H.D. Kaesz, J. Organomet. Chem., 191 (1980) 243.
12 G.R. Crooks, B.F.G. Johnson, J. Lewis and I.G. Williams, J. Chem. Soc. (A), (1969) 797.
13 S. Jeannin, Y. Jeannin, G. Lavigne, Inorg. Chem., 17 (1978) 2103.
14 D. Enders and H. Eichauer, Chem. Ber., 112 (1976) 2933.
15 M.I. Bruce, D.C. Kehoe, J.G. Matisons, K.B. Nicholson, P.H. Rieger and M.C. Williams, J. Chem. Soc., Chem. Commun., (1982) 442.
16 M.I. Bruce, T.W. Hambley, K.B. Nicholson and M.R. Snow, J. Organomet. Chem., 235 (1982), C57, 83.
17 G.M. Sheldrick, SHELX Program for crystal structure determination, University of Cambridge, 1976.
18 International Tables for X-Ray Crystallography, Kynoch Press, Birmingham, 1974, Vol. 4.